

Noise propagation from pump to secondary lasers

A. W. Yu

School of Physics, Georgia Institute of Technology, Atlanta, Georgia 30332

Govind P. Agrawal

AT&T Bell Laboratories, Murray Hill, New Jersey 07974

R. Roy

School of Physics, Georgia Institute of Technology, Atlanta, Georgia 30332

Received May 26, 1987; accepted July 28, 1987

Experimental measurements of the intensity fluctuations and the associated power spectra for the pump (argon) laser and the secondary (dye) laser show that the secondary laser follows pump fluctuations when operated far above threshold but acts as a low-pass filter when operated close to threshold. The experimental results are well explained by a laser model that accounts for pump fluctuations through a multiplicative colored-noise process. The theory and the experiment are in good quantitative agreement.

Secondary lasers, i.e., those in which the excitation of the active medium is provided by another primary laser, have rapidly gained importance in the last decade. Examples of this type of laser are organic dye, F center, alexandrite, titanium-doped sapphire, and YAG lasers. The primary or pump lasers employed to invert these active media are argon, krypton, and semiconductor lasers. The output power of the secondary laser depends on the input pump power. In addition, any noise that is present in the pump laser can be expected to influence the intensity and phase noise of the secondary laser. Stochastic pump noise has been found to be a source of anomalously large fluctuations in dye lasers.¹ Previous studies of pump noise in dye lasers have concentrated on the intensity autocorrelation function.¹⁻⁷ The transient behavior of the laser was studied⁸; a technique based on the concept of the first-passage time was developed to obtain estimates of the strengths and time scales of the noise sources present in the dye laser.

In this Letter we examine the power spectra of the pump and secondary lasers directly for the specific case of a dye laser pumped by an argon laser. In particular, we investigate the transfer of the pump-laser noise to the output of the dye laser. Our experiments show that the secondary laser reproduces fluctuations of the pump laser with greater accuracy as it is pumped increasingly above threshold. However, at operating points near threshold, the secondary laser behaves as a low-pass filter for pump-laser fluctuations. A theoretical explanation of this behavior is presented based on a laser model that includes pump fluctuations through a multiplicative colored-noise process^{3,7} together with the spontaneous-emission-induced quantum noise.

A ring dye laser pumped by an intensity-stabilized argon laser (514.5 nm) is operated unidirectionally in a single longitudinal and transverse mode. The dye laser is vibration isolated; an enclosure protects it from air currents and dust. The mode structure of the

laser field is monitored with a confocal Fabry-Perot interferometer to ensure that the laser operates in a single mode. A small fraction of the argon-laser beam is split off before it becomes incident upon the dye jet and is monitored by a fast photodiode (rise time <1 nsec). A fraction of the dye-laser output is similarly monitored. The two signals are displayed simultaneously on a dual-beam digital oscilloscope that is used to digitize and store these signals. Several thousand digitized values of the laser intensities can be stored and fast Fourier transformed to obtain the power spectra of intensity fluctuations.

In Fig. 1 we show traces of the pump- and dye-laser signals. The dye-laser output is 15 mW, and its fluctuations are seen to correspond closely to those of the pump laser, on the time scale shown. In Fig. 2 the corresponding power spectra of the argon and dye lasers are shown. The lower traces are for the range 0-6.22 MHz, whereas the upper ones are expanded ver-

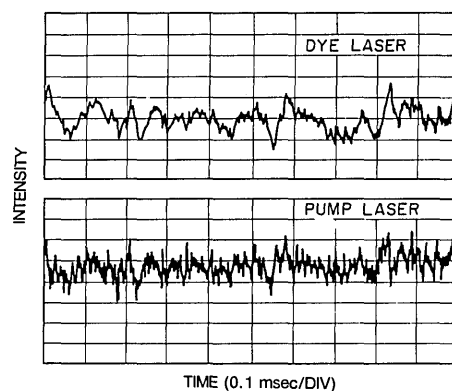


Fig. 1. Time traces of the intensity fluctuations of the pump and dye lasers. The dye-laser output power was ≈ 15 mW for a pump-laser power of ≈ 2 W. The rms fluctuation is about 2 and 10% of the dc level for the argon and dye lasers, respectively.

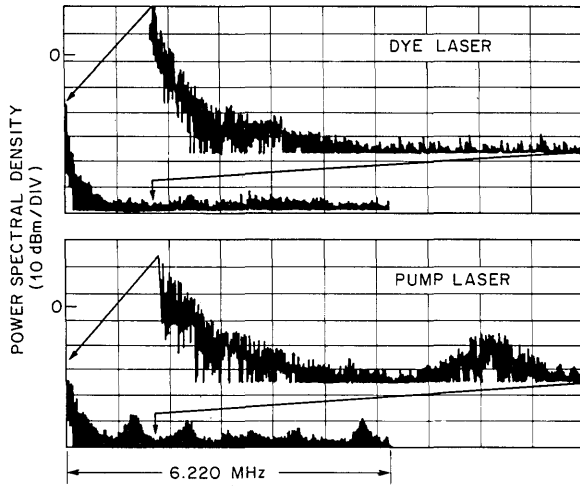


Fig. 2. Power spectra of the time traces shown in Fig. 1 for pump and dye lasers obtained by Fourier transforming the digitized data (12,500 points). The upper trace in each case shows the low-frequency region on an expanded scale in the range 0–1.8 MHz.

sions of the low-frequency segments from 0 to 1.8 MHz. The power spectrum of the dye laser is limited to about 1 MHz. The power spectrum of the argon laser has a main peak extending to ~ 1 MHz, but it also exhibits subsidiary peaks at 1.2 MHz and higher frequencies. We note that the argon laser is intensity stabilized and its spectrum does not display any frequency components at 60 Hz or its multiples. If the laser is run under the current control mode, the power spectra of both the argon and the dye lasers show peaks at 60 Hz together with a large number of harmonics.

As the dye laser is operated progressively closer to threshold, the correspondence between the pump- and secondary-laser fluctuations is seen to decrease, until at about 1 mW the dye-laser output shows a minimal resemblance (Fig. 3). The pump-laser spectrum is virtually unchanged, since only a small reduction in pump power is required to reduce the dye-laser output from 15 to 1 mW. The power spectra corresponding to the traces of Fig. 3 are shown in Fig. 4. The dye-laser spectrum is now restricted to a much smaller range of frequencies than that in Fig. 2. The expanded range of the spectrum covers the range from 0 to 0.45 MHz. The dye-laser intensity noise is thus appreciable only in the region < 0.2 MHz. In what follows we give a simple theoretical model to explain these observations.

To interpret the results of these experiments, we take the model^{3,7} of the dye laser with multiplicative noise as our starting point. Such a model was found appropriate to include the effect of pump noise for the calculation of both the steady-state and the transient phenomena. The equation for the electric field of the secondary laser is written as

$$\dot{E} = a_0 E - A|E|^2 E + p(t)E + q(t), \quad (1)$$

where $p(t)$ is a colored-pump-noise term and $q(t)$ is a delta-correlated quantum-noise term. The electric field E is complex and dimensionless.⁸ The param-

eter a_0 is the net gain of the laser, while A is the saturation coefficient. The statistical properties of the quantum and pump noise are given by

$$\langle q(t)q^*(t') \rangle = 2R\delta(t - t'), \quad (2)$$

$$\langle p(t)p^*(t') \rangle = D\Gamma_p \exp(-|t - t'|\Gamma_p), \quad (3)$$

where R and D are the strengths of the quantum and pump noise and $1/\Gamma_p$ is the time scale of the pump noise.

Instead of the complex electric field, Eq. (1) can be used to obtain the following equation for the laser intensity $I = |E|^2$:

$$dI/dt = 2a_0 I - 2AI^2 + R + 2p_r(t)I + 2q_r(t)\sqrt{I}, \quad (4)$$

where the subscript r denotes the real part. A linearized analysis of the intensity fluctuations can now be performed by letting

$$I(t) = \bar{I} + \delta(t), \quad (5)$$

where \bar{I} is the average steady-state intensity. Above threshold, the average steady-state intensity is given to a good approximation $\bar{I} \approx a_0/A$. Linearizing Eq.

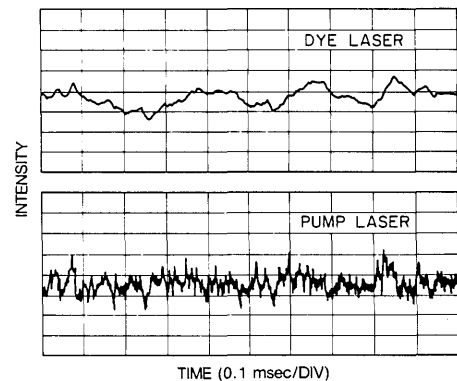


Fig. 3. Same as in Fig. 1, but at a lower dye-laser power of about 1 mW. The pump-laser power is nearly the same (≈ 2 W). The rms fluctuation is about 2 and 30% of the dc level for the argon and dye laser, respectively.

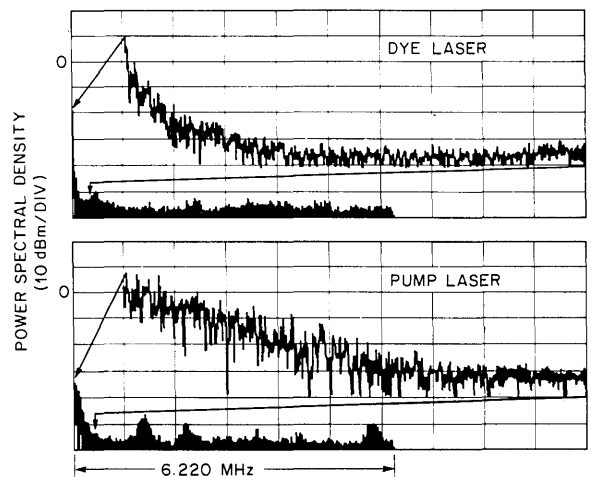


Fig. 4. Power spectra of the time traces shown in Fig. 3 for pump and dye lasers. The upper trace in each case shows the low-frequency region on an expanded scale in the range 0–0.45 MHz.

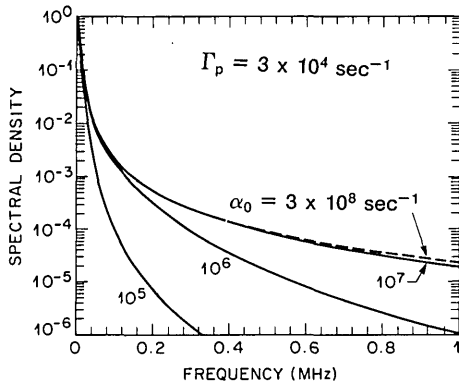


Fig. 5. Calculated power spectra (normalized) for the dye-laser fluctuations for several values of the net gain coefficient a_0 .

(4) in $\delta(t)$, we obtain

$$\dot{\delta}(t) = \left[2a_0 - 4A\bar{I} + 2p_r(t) + \frac{q_r(t)}{\sqrt{\bar{I}}} \right] \delta + 2q_r(t)\sqrt{\bar{I}} + 2p_r(t)\bar{I}. \quad (6)$$

If we neglect the fluctuating terms in comparison with $2a_0 - 4A\bar{I}$, we may conveniently solve Eq. (6) in the Fourier domain and obtain

$$\tilde{\delta}(\omega) = [2\bar{I}\tilde{p}_r(\omega) + 2\tilde{q}_r(\omega)\sqrt{\bar{I}}]/(2a_0 + i\omega). \quad (7)$$

where the tilde denotes the Fourier transform. This assumption is appropriate for the experiments reported here, which were performed in the regime above threshold, but a more complete theory is necessary if the laser-threshold region is to be included. The power spectrum of the secondary-laser intensity fluctuations is obtained using Eqs. (2), (3), and (7):

$$S(\omega) = \langle |\tilde{\delta}(\omega)|^2 \rangle = \frac{4\bar{I}R}{(\omega^2 + \Gamma_L^2)} + \frac{(D/A^2)\Gamma_L^2\Gamma_p^2}{(\omega^2 + \Gamma_L^2)(\omega^2 + \Gamma_p^2)}, \quad (8)$$

where

$$\Gamma_L = 2a_0. \quad (9)$$

The structure of the spectrum is quite interesting and provides a direct explanation of our experimental observations. The first term, involving the quantum noise, is negligible for operation above threshold. This is clear from the relative magnitudes of the noise strengths R and D , as determined from our previous experiments ($R/D < 10^{-6}$).⁸ The second term is a product of two Lorentzians. One of them is the spectrum of the pump noise that we have assumed to be Lorentzian with parameter Γ_p , while the second has a width determined by the parameter a_0 . The shape of the resultant spectrum will clearly depend on the relative widths of these two Lorentzians.

To compare theory with experiment, we need estimates of Γ_L and Γ_p . From Eq. (9) Γ_L is determined by the parameter $a_0 = G - \kappa$, where G is the gain and κ is the cavity decay rate ($\kappa \simeq 1 \times 10^7 \text{ sec}^{-1}$ for the dye laser used in the experiment). At threshold, $G = \kappa$ and consequently $a_0 = 0$. Above threshold, $a_0 = \kappa\eta$, where

$\eta = G/\kappa - 1$ is the relative excitation. Thus, for operation 10% above threshold, $\eta = 0.1$ and $a_0 = 1 \times 10^6 \text{ sec}^{-1}$. We estimated Γ_p from the pump-power spectrum shown in Fig. 2. By fitting the observed spectrum with a Lorentzian, we estimate that $\Gamma_p \simeq 3 \times 10^4 \text{ sec}^{-1}$.

Figure 5 shows the calculated power spectra obtained by using Eq. (8) for several values of a_0 . For $\eta \gg 1$, the power spectrum becomes nearly independent of a_0 . This can be understood from Eq. (8) by noting that $S(\omega)$ becomes independent of Γ_L for $\Gamma_p \ll \Gamma_L$. In other words, far above threshold, the power spectrum is completely determined by the pump noise, in agreement with our experimental observations. For operation closer to threshold, Γ_L is comparable with Γ_p , and the predicted power spectrum is narrower than the simple Lorentzian expected from the pump noise alone. This is shown in Fig. 5 by the curve for $a_0 = 1 \times 10^5 \text{ sec}^{-1}$, which should be compared with the observed power spectrum shown in the top panel of Fig. 4 (1 mW of dye-laser output corresponds to $\eta \simeq 0.01$). Thus the simple colored-noise model is capable of explaining our experimental observations. Furthermore, the predicted spectral width of the dye-laser power spectrum is in good quantitative agreement with the experimental data in Figs. 2 and 4 obtained for $a_0 \simeq 10^6 \text{ sec}^{-1}$ and $a_0 \simeq 10^5 \text{ sec}^{-1}$, respectively. It should be emphasized that no fitting parameter was used to compare theory with experiment. The close agreement between the two reinforces the validity of the multiplicative colored-noise model for dye lasers, in particular, and for optically pumped secondary lasers, in general.

To conclude, we investigated the dependence of the power spectrum of a secondary laser on that of the primary or pump laser. The secondary laser is seen to behave as a low-pass filter when operated near threshold but reproduces the pump-laser fluctuations more faithfully when it is run at higher excitations. The experimental observations were explained by calculations of the power spectrum based on a theoretical model of a secondary laser with a stochastic pump. These results should apply to any secondary laser and are therefore relevant to the operation of a wide variety of laser systems in use today.

The work at Georgia Tech was supported by a grant from the U.S. Department of Energy, Office of Basic Energy Sciences, Chemical Sciences Division.

References

1. K. Kaminishi, R. Roy, R. Short, and L. Mandel, *Phys. Rev. A* **24**, 370 (1981).
2. R. Graham, M. Hohnerbach, and A. Schenzle, *Phys. Rev. Lett.* **48**, 1396 (1982).
3. S. Dixit and P. Sahni, *Phys. Rev. Lett.* **50**, 1273 (1983).
4. R. F. Fox, G. E. James, and R. Roy, *Phys. Rev. A* **30**, 2482 (1984).
5. A. Hernandez-Machado, M. San Miguel, and S. Katz, *Phys. Rev. A* **31**, 2362 (1985).
6. P. Jung and H. Risken, *Z. Phys. B* **59**, 469 (1985).
7. R. F. Fox and R. Roy, *Phys. Rev. A* **35**, 1838 (1987).
8. S. Zhu, A. W. Yu, and R. Roy, *Phys. Rev. A* **34**, 4333 (1986).